INFLUENCE OF INTACT ROCK STRENGTH ON ROCK MASS MECHANICAL PROPERTIES

*K. Esmaieli, J. Hadjigeorgiou, and N. Layos
Lassonde Institute of Mining, University of Toronto
170 College Street
Toronto, Canada M5S 3E3
*(*Corresponding author: Kamran.esmaeili@utoronto.ca)*

INFLUENCE OF INTACT ROCK STRENGTH ON ROCK MASS MECHANICAL PROPERTIES

ABSTRACT

The Synthetic Rock Mass (SRM) approach has the potential to capture the mechanical behavior of large rock samples. In order for the method to be used with confidence it is necessary to gain a good understanding of the factors that influences its analysis. This paper reports on a series of numerical experiments, based on field data from a large underground mine, to investigate the influence of intact rock mass strength of a constructed (SRM). A jointed rock mass defined by three fracture sets was simulated by a Discrete Fracture Network (DFN) model. The generated fracture network was subsequently embedded into six different intact rock samples, simulated by a bonded particle model in PFC3D, generating six SRM samples. Each intact rock sample was 7 m × 7 m × 14 m and assigned different mechanical properties. The first intact rock sample was assigned a uniaxial compressive strength of 205 MPa and an elastic modulus of 104 GPa with the UCS and elastic modulus values of the other samples downgraded by 10% until the weakest sample had a UCS value of 121 MPa and an elastic modulus value of 61 GPa. All SRM samples were loaded under uniaxial compression to obtain the complete stress strain curve. It was observed that the compressive strength of the rock mass samples decreased by 10% following the same trend as the rock material strength. However, the elastic modulus of the rock mass samples decreased non-linearly with reduction of the elastic modulus of the rock material. The Poisson's ratio of rock mass samples does not change with decrease of rock material properties. For the post-peak behaviour the results show that both the brittleness index and the residual strength of rock mass samples decreased as the rock material properties degrades.

KEYWORDS

Intact rock properties, Rock mass mechanical behaviour, Synthetic Rock Mass (SRM), Discrete Fracture Network (DFN), PFC3D

INTRODUCTION

The mechanical properties of a rock mass are controlled by multitude of parameters including the continuity, orientation and frequency of fractures in the rock mass and the fracture surface characteristics. Empirical assessments of rock mass mechanical properties often rely on a classification approach (i.e. Rock Mass Rating (RMR), Geological Strength Index (GSI), Q system), where several parameters are grouped together to identify a unique index of rock mass quality. There are several empirical equations that use a classification index to degrade the intact rock strength and elastic modulus, (Barton 2002; Hoek & Diederichs 2006; Hoek et al. (2002); Kalamaras & Bieniawski (1995); Sonmez et al. 2004). This approach has been extended to estimate the post peak behavior of rock mass using the GSI systems, (Cai et al. 2006). The inherent assumption is that the highest rating in a classification system corresponds to the intact rock conditions. Although this approach is convenient it is recognized that the constitutive case studies of these classification systems were never intended to provide an indication of strength or deformation.

The numerical Synthetic Rock Mass (SRM) methodology allows for a quantitative approach to estimate the strength and deformability of large-scale rock samples, (Esmaieli et al. 2010; Mas Ivars et al. 2010). Use of SRM technology is however evolving as we address the impact of different assumptions in constructing SRM models. This paper illustrates the impact of intact rock properties to the simulated behavior of jointed rock mass as represented by large SRM samples. The numerical experiments use data collected from a site investigation at Brunswick Mine, a large underground mine in New Brunswick, Canada.

DFN MODELING

Data Collection

Structural data were collected from six scan-lines in drifts at the 1000 and 1225 levels, in the lower block of Brunswick Mine. Analysis of field data collected in these massive sulphides identified two sub-vertical fracture sets relatively perpendicular to each other (set #1 and set #2), directed along East-West and North-South, and one sub-horizontal fracture set (set #3) which has less dispersion compared to the other fracture sets, Table 1. The statistical distribution of the orientation, spacing and trace length data for the three fracture sets were tested using the Kolmogorov- Smirnov test. The results of the K-S tests indicated the Fisher univariate distribution for the fracture sets orientation data, the exponential distribution for the fracture sets spacing data and the lognormal distribution for the trace length data of fracture sets, (Esmaieli et al. 2010). A DFN was constructed using the input data summarised in Table 1.

Table 1- Summary of fracture set characteristics measured in the field.

Fracture Set #	Orientation			Normal Set Spacing		Trace Length	
	Dip	Dip Dir	K	Mean (m)	Std.	Mean (m)	Std.
1	89	007	17	1.52	1.8	1.81	0.73
2	89	274	12	1.12	1.0	1.69	0.54
3	17	227	57	1.23	0.8	1.23	0.22

DFN Model Generation and Validation

Stochastic models for representation of fracture network have found many applications in rock engineering including mining, civil, environmental and reservoir engineering. Discrete Fracture Network (DFN) models are generated based on specific relationships between fracture characteristics such as orientation of fracture sets, fracture shape, size, and termination, (Dershowitz & Einstein, 1988).

The Discrete Fracture Network (DFN) model for the massive sulphide rock mass at Brunswick Mine was generated using the Fracture-SG generator, developed by (Grenon & Hadjigeorgiou, 2008). This code is based on the Veneziano model. For DFN model generation, statistically analyzed field data including the information about fracture sets orientation, trace length and spacing are employed as necessary input data. The DFN model generation is an iterative process that is repeated until statistical agreement is reached between the field data and simulated data. Figure 1a shows a DFN model of 40 m × 40 m × 40 m for the massive sulphide rock mass at Brunswick Mine. This is only one possible representation of the model, populated with 72816 fracture polygons. The fracture set #1, set #2 and set #3 were identified with red, blue and green color, respectively. The Y-axis in the Figure representing North. Once the DFN model was validated, a cubic sample of 7 m x 7 m x 14 m was randomly extracted from within the initial master DFN model, Figure 1b.

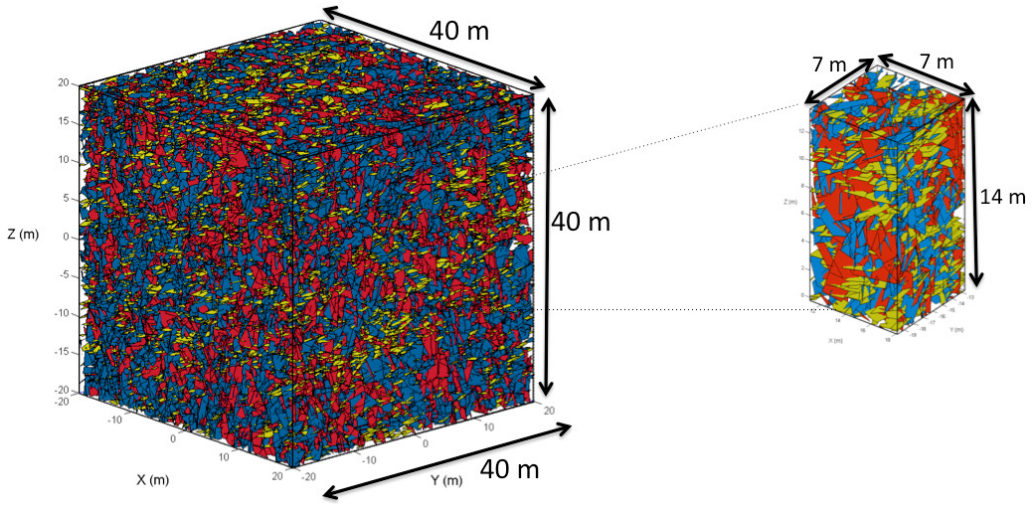

Figure 1- a) Master DFN model, b) A DFN sample of 7 m x 7 m x 14 m randomly extracted from the mater model. (Note: the figures are not to scale).

GENERATION OF THE SYNTHETIC ROCK MASS SAMPLES

Simulation of Intact Rock

For the purposes of this study, six intact rock samples were simulated using the bonded particle model, presented by (Potyondy & Cundall, 2004). The BPM simulates an intact rock as a packing of non-uniform circular or spherical rigid particles that are connected together at their contact points with parallel bonds. The micro mechanical properties of the rigid particles are shear and normal stiffness and coefficient of friction. The micro-properties of the parallel bonds are normal and shear stiffness, tensile and shear strength and parallel bond radius multiplier.

An inverse calibration method was used to establish the appropriate micro-mechanical parameters of a BPM that will result in representative intact rock properties. The assigned mechanical properties of intact rock in a bonded particle model were compared to the results of mechanical properties from laboratory tests to those obtained from computational tests.

The geomechanical properties of the massive sulphide rock at the Brunswick Mine was used as the mechanical properties of the first intact rock sample. This sample was assigned a uniaxial compressive strength (UCS) of 205 MPa and an elastic modulus of 104 GPa. Five more samples were generated in sequence by downgrading the UCS and elastic modulus values each time by 10%. Figure 2 presents the six intact rock samples and their mechanical properties (UCS and Elastic modulus). The Poisson's ratio of all the samples was fixed at 0.27. An inverse calibration method was used to establish the necessary micro-mechanical parameters that would replicate the representative intact rock properties. The UCS of the intact rock samples varied from 121 to 205 MPa, while the elastic modulus of was from 62 GPa to 104 GPa. All intact rock samples were generated with a fixed size of 7 m x 7m x 14 m.

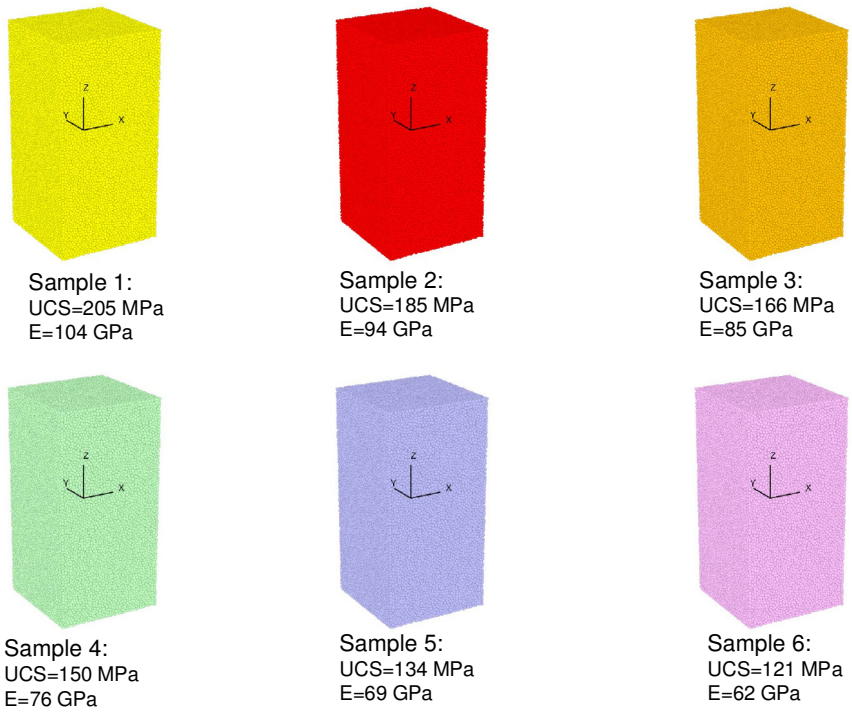

Figure 2. Six intact rock samples generated using BPM.

Fracture Properties

A bonded particle model can represent a homogeneous rock but it can also be divided into a number of discrete regions, or blocks by discrete fracture planes. The properties of particles and bonds along the fracture planes are usually different than those that exist in the solid part of the model. For the purposes of this work the smooth joint model (SJM) was applied to the particle contacts. This ensures sliding and unraveling of rock blocks along the fracture surface. All fractures were assumed to be cohesionless and having an angle of friction of 30^{o}. The calibration process described by (Esmaieli et al., 2010) was used to assign the necessary micro-mechanical properties to the particles along the fracture planes, in order to achieve the desired fracture macro- properties.

SRM Sample Generation

A synthetic rock mass (SRM) model uses the Particle Flow Code to represents a jointed rock mass as an assembly of fractures inserted into a rock matrix. The SRM approach, developed by (Pierce et al., 2007) necessitates a link between a DFN model and a bonded particle model. The fractures are represented in the BPM where a smooth joint model is applied to particle contacts along the fracture planes. Loading of a SRM model can result in new fracture initiation and propagation and sliding along pre-existent fractures.

The same 7 m x 7 m x 14 m DFN model was superimposed on the six intact rock samples to construct six unique SRM samples. Figure 3 presents the SRM sample generated for the sample 1. All six SRM samples were uniaxially loaded to estimate the mechanical behaviour of the samples.

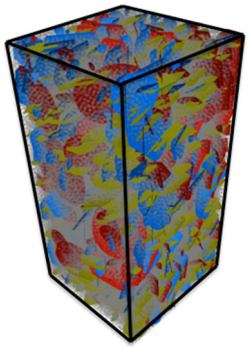

Figure 3- An example of SRM sample generated by linking the DFN model with the intact rock sample 1.

RESULTS

Stress-Strain Behaviour

Figure 4 shows a typical stress-strain curve for a strain softening material (i.e. moderately fractured hard rock masses). Five zones can be identified in the stress-strain curve including: elastic, yielding, brittle, softening and residual phase. In routine testing applications only the elastic and yielding phases are recorded. The complete stress-strain behaviour of a loaded sample can be determined using stiff servo-controlled press (Hudson et al., 1971). Nevertheless there is very limited experimental data on the complete stress strain behaviour for large samples.

An indication of the behaviour of large samples can be derived from back analyses of cases studies through numerical modeling. This is not a trivial problem in most cases due to the inherent model complexity. Another approach is to extrapolate from small-scale samples using some form of degradation aiming to account for what is referred to as the scale effect.

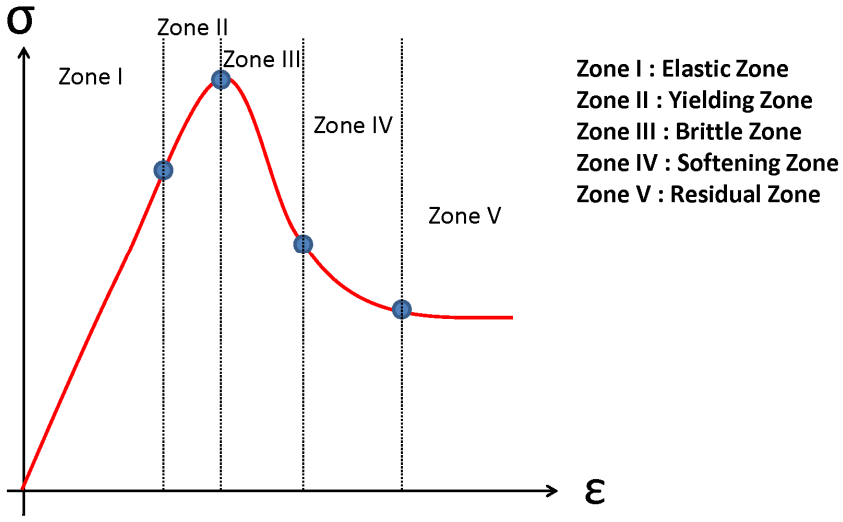

Figure 4- Idealised stress-strain curve for a strain softening material.

The six SRM samples were loaded under uniaxial compression following the procedures in (Esmaeili et al., 2010), Figure 5.

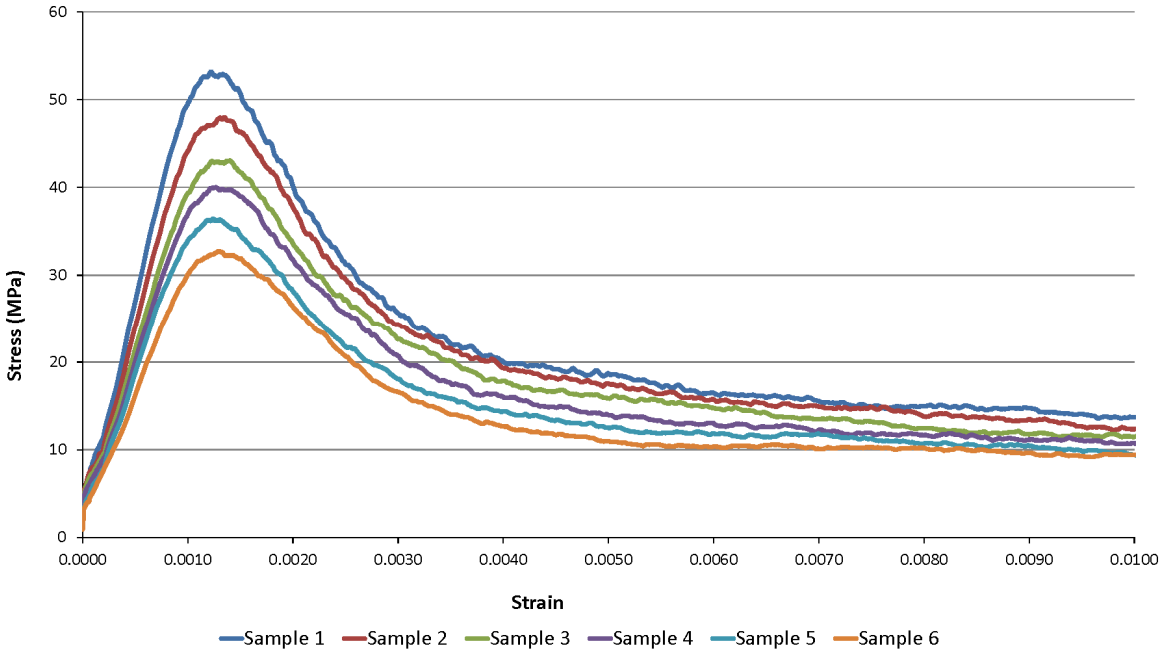

Figure 5- Stress-strain curves for the six SRM samples.

It can be seen that all six samples under uniaxial loading follow the stress strain behaviour of a strain softening material. It is possible to interpret these numerical test results to assign material properties in a similar way as in standardised laboratory tests, Table 2. The present investigation has focused on exploring the influence of the strength of intact rock in a rock mass matrix on the resulting strength of a synthetic rock mass.

Table 2- The mechanical properties of the intact rock samples and the SRM samples.

Sample #	Intact Rock Properties			Rock Mass Properties					
				Pre-peak properties				Post peak properties	
	UCS (MPa)	E (GPa)	Poisson's Ratio	UCS (MPa)	E (GPa)	Poisson's Ratio X	Poisson's Ratio Y	Post Peak Modulus (GPa)	Residual Strength (MPa)
1	205	104	0.27	53	47.3	0.45	0.48	-20.8	13.0
2	185	94	0.27	48	41.0	0.46	0.48	-17.4	12.0
3	166	85	0.27	43	36.0	0.46	0.49	-16.5	11.0
4	150	76	0.27	40	32.7	0.46	0.47	-13.6	10.5
5	134	69	0.27	36	30.6	0.45	0.46	-12.2	10.0
6	121	62	0.27	33	28.1	0.45	0.48	-10.2	9.4

Pre-Peak Mechanical Properties

Uniaxial Compressive Strength

The results of the numerical models indicate that reducing of the intact rock strength decreases the uniaxial compressive strength of the SRM samples. Figure 6 presents the linear relationship between the

UCS of the intact rock and the UCS of the Synthetic Rock Mass samples. The Figure indicates that reducing of the rock material strength by 10% constitutively will decrease the UCS of the rock mass samples by 7% to 10%. For all the SRM samples, the UCS of rock mass is about 26% of the UCS of the intact rock samples. It should be noted that all SRM samples had the same structural properties (joint orientation, spatial distribution, properties, etc.).

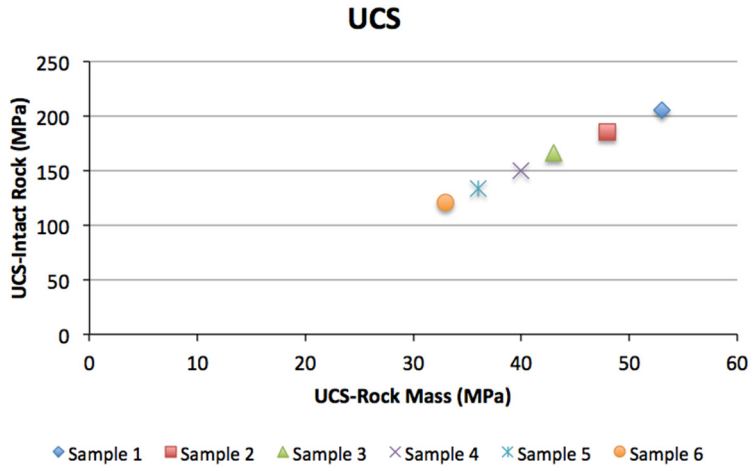

Figure 6. The relationship between the UCS of the rock material and the UCS of the SRM samples.

Elastic Modulus

The elastic modulus of the SRM samples was estimated for the uniaxial loading tests using the secant method. Figure 7 presents the relationship between the elastic modulus of the SRM samples and the elastic modulus of the intact rock. The Figure illustrates that, the elastic modulus of the rock mass samples decreases non-linearly with a reduction in the elastic modulus of the intact rock. The Figure shows that reducing the deformation modulus of rock material by 10% constitutively downgrades the deformability of the fractured rock mass samples by 6% to 13%. The ratio of the elastic modulus of the SRM samples per the elastic modulus of the intact rock samples is varying between 42% and 46%.

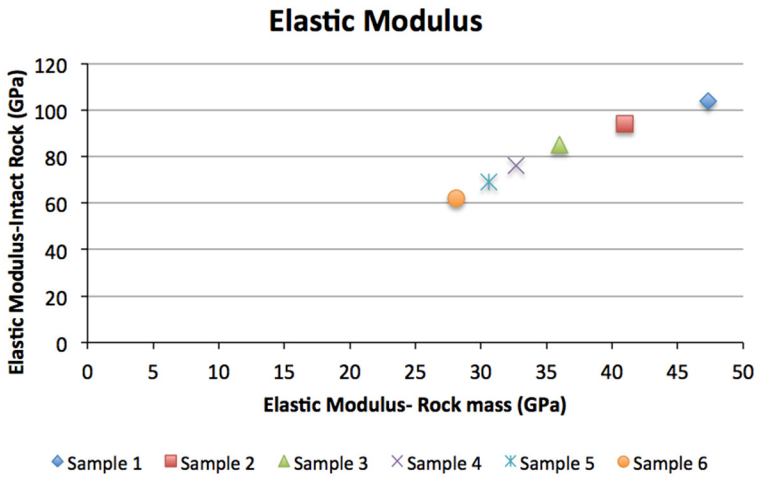

Figure 7- The relationship between the elastic modulus of the intact rock material and the elastic modulus of the SRM samples.

Poisson's Ratio

The Poisson's ratio of the SRM samples was measured along both the xx and yy directions, during the uniaxial loading. Figure 8 shows the relationship between the Poisson's ratio of intact rock samples and the SRM samples. The results indicate that although the Poisson's ratio of rock material remains constant at 0.27, the Poisson's ratio of the rock mass samples varying from 0.44 to 0.49. Higher Poisson's ratio values were recorded along the yy direction (North-South direction). This can reflect the variation of the fracture frequency and the size of fractures in the North-South direction versus the East-West direction.

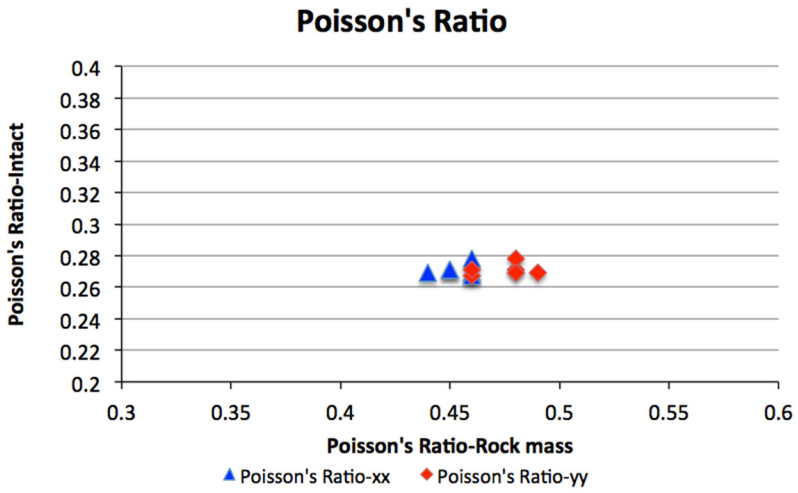

Figure 8- The relationship between the Poisson's ratio of the rock material and the Poisson's ratio of the SRM samples in xx and yy direction.

Post-Peak Mechanical Properties

The post peak behaviour of a sample is influenced by material properties but also by the testing procedure. A convenient way to compare the post peak behaviour of different rock samples is through the use of the brittleness index.

Brittleness Index

To quantify rock brittleness in compression conditions of σ1 > σ2 = σ3, Tarasov (2010) proposed a brittleness index k (equation 1). This index is based on the elastic energy accumulated in the rock during loading, and the portion of this energy that cause failure development in the post-peak phase.

$$k = \frac{dW_r}{dW_e} = \frac{E - M}{M} \qquad (1)$$

Where:

$dW_r = \frac{d\sigma^2(E-M)}{2EM}$ is the rupture energy; $dW_e = \frac{d\sigma^2}{2E}$ is the accumulated elastic energy available for the rupture process; $E = \frac{d\sigma}{d\varepsilon}$ is the unloading elastic modulus; $M = \frac{d\sigma}{d\varepsilon}$ is the post-peak modulus.

The parameters of the equation (1) can be determined from complete stress–strain curves. Tarasov (2010) demonstrated the variation in brittleness index with variation of complete stress-strain curves, Figure 9. The brittleness index k increases from left to right. In this Figure it was assumed that pre-peak parts of the curves are the same. The brittleness index is negative ranging from $-\infty < k < 0$.

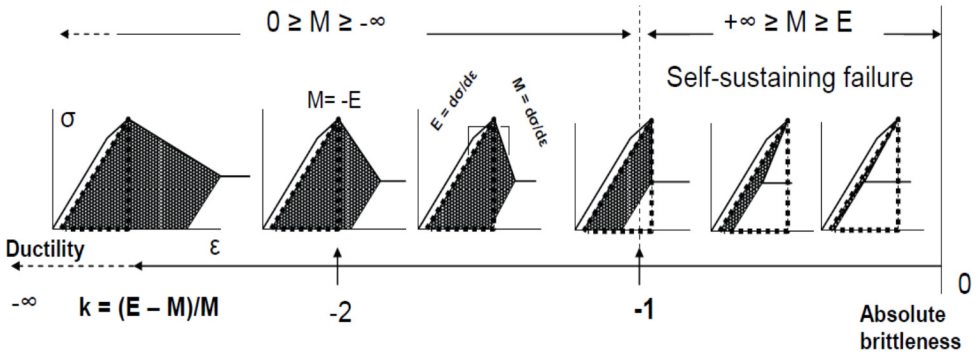

Figure 9- Variation of brittleness index (k) with characteristic shape of complete stress-strain curves, (Tarasov, 2010).

Using the definition proposed by (Tarasov, 2010), the brittleness index was calculated for all tested SRM samples using the elastic modulus and post peak modulus of the different samples, Figure 10.

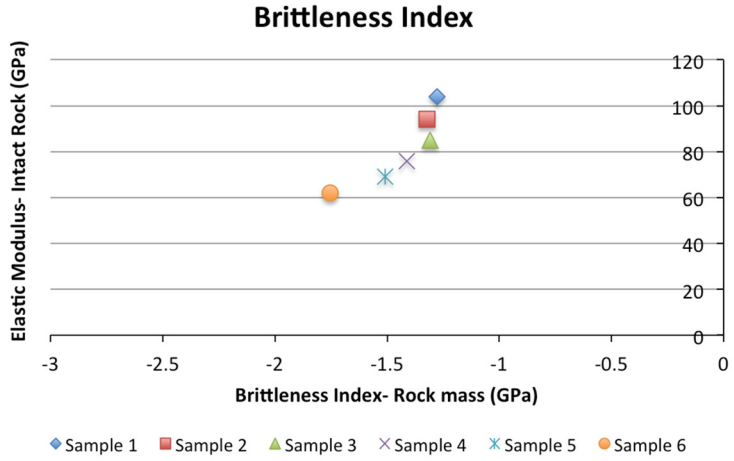

Figure 10- Influence of rock material properties on the brittleness index of the SRM samples.

The graph indicates that the brittleness index diminishes significantly with decreasing of rock material properties. The index varies between $-1.75 < k < -1.27$. This implies that by reducing the rock material properties, the rock mass becomes more ductile.

Residual Strength

The residual strength of the SRM samples was calculated based on Figure the stress strain curves plotted in Figure 5. Figure 11 presents the relationship between the strength of the rock material matrix and the residual strength of the rock mass. The results show that reducing the rock material properties decreases the residual strength of the rock mass. For all the SRM samples, the ratio of the residual strength of rock mass sample per the ultimate strength of rock mass sample remains constant (Rock Mass Residual Strength/Ultimate Rock Mass Strength = 0.27).

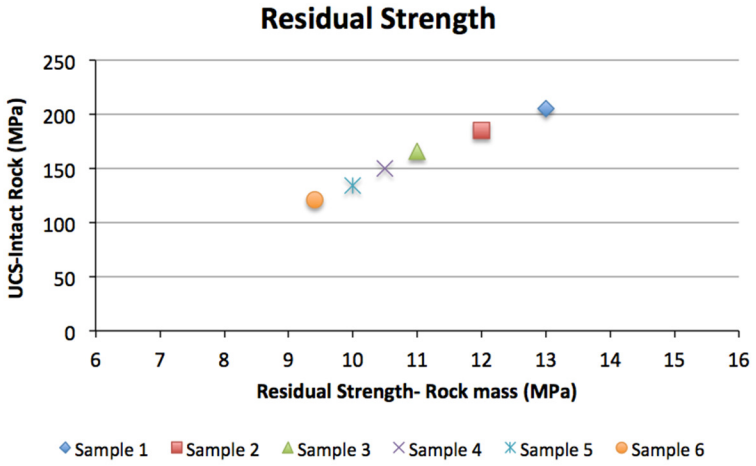

Figure 11- Influence of rock material strength on the residual strength of rock mass.

CONCLUSIONS

SRM technology can provide useful insights into the behaviour of large rock samples. The process is influenced by the type and number of assumptions in constructing SRM models. The paper presented a quantitative approach to estimate the sensitivity of pre-peak and post-peak behaviour of a SRM to the intact rock properties used in the model. Field data were collected to generate a representative DFN model for a massive sulphide rock mass. A large sample of 7 m x 7 m x14 m was randomly collected from the master DFN model. Six intact rock samples of the same size were generated using the bonded particle model. Different UCS and elastic modulus values were assigned to each sample, with 10% difference between two consecutive samples. All six samples were loaded under a uniaxial compressive force and the pre-peak and post-peak behavior of the rock masses were estimated.

The numerical experiments suggested that both the strength and deformability of rock mass decreases with the reduction of intact rock strength and deformability. However, contrary to the linear relationship between the UCS of intact rock and the UCS of rock mass, the relationship between the deformability of rock mass and the deformability of intact rock is non-linear. In addition, no relationship was observed between the Poisson's ratio of intact rock and that of the fractured rock mass samples. For the post-peak behavior, the residual strength of fractured rock mass samples reduces by decreasing the UCS of the intact rock. Finally, degrading the mechanical properties of rock matrix can make the synthetic rock mass behavior more ductile.

ACKNOWLEDGEMENTS

The authors would like to acknowledge the financial support of the Natural Science and Engineering Research Council of Canada.

REFERENCES

Barton, N. (2002). Some new Q value correlations to assist in site characterization and tunnel design. *Int. J. Rock Mech. Min. Sci.*, 39:185-216.

Cai, M., Kaiser, P.K., Tasaka, Y., Minami, M., (2006). Determination of residual strength of jointed rock masses using the GSI system. *Int. J. Rock Mech. Min. Sci.* doi. 10.1016/j.ijrmms.2006.07.005.

Dershowitz, W.S., Einstein, H.H. (1988). Characterizing rock joint geometry with joint system models. *Rock Mech. Rock Eng.* 21: 21-51.

Esmaieli, K., Hadjigeorgiou, J. & Grenon, M. (2010). Estimating geometrical and mechanical REV based on synthetic rock mass models at Brunswick Mine. *Int. J. Rock Mech. Min. Sci.* doi.10.1016/j.ijrmms.2010.05.010.

Grenon, M., & Hadjigeorgiou, J. (2008). Fracture-SG. A fracture system generator software package, Version 2.17.

Hoek, E., Carranza-Torres, C.T., Corkum, B. (2002). Hoek-Brown failure criterion-2002 edition. In Proceedings of the fifth north American rock mechanics symposium, Toronto, p.267-273.

Hoek, E., Diederichs, M.S., (2006). Empirical estimation of rock mass strength. *Int. J. Rock Mech. Min. Sci.* 43, 203-215.

Hudson, J.A., Brown, E.T. & Fairhust, C. (1971). Optimizing the control of rock failure in servo-controlled laboratory test. *Journal of Rock Mechanics,* 3, 217-224.

Kalamaras G.S., Bieniawski, Z.T. (1995). A rock mass strength concept for coal incorporating the effect of time. In Proceeding of the eight international congress of the rock mechanics, Rotterdam, Balkema, p. 295-302.

Mas Ivars, D., Pierce, M., Darcel, C., Reyes-Montes, J., Potyondy, D.O., Young, P., Cundall, P.A., (2010). The synthetic rock mass approach for jointed rock mass modeling. *Int. J. Rock Mech. Min. Sci.* doi.10.1016/j.ijrmms.2010.11.014.

Pierce, M., Mas Ivars, D., Cundall, P.A. & Potyonday, D. (2007). A synthetic rock mass model for jointed rock. In proceedings of the first Ca-US rock mechanics Symposium, Vancouver, 2007, p.341-349.

Potyondy, D., Cundall, P.A. (2004). A bonded particle model for rock. *Int. J. rock Mech. Min. Sci.* 41: 1329-1364.

Sonmez, H., Gokceoglu, C., Ulusay, R., (2004). Indirect determination of the modulus of deformation of rock masses based on the GSI system. *Int. J. Rock Mech. Min. Sci.* 41, 849-857.

Tarasov, B.G. (2010). Superbrittleness of rocks at high confining pressure. In proceeding of *Fifth International Seminar on Deep and High Stress Mining,6-8 October 2010, Santiago, Chile.*